Varactor-Loaded Transmission-Line Phase Shifter at C-Band Using Lumped Elements

Frank Ellinger, *Member, IEEE*, Heinz Jäckel, *Member, IEEE*, and Werner Bächtold, *Fellow, IEEE*

***Abstract*—The design of varactor-loaded transmission-line phase shifters using lumped elements is discussed in this paper. A monolithic-microwave integrated-circuit phase shifter is fabricated to verify the proposed topology. Only one control voltage is required for phase control. Within a continuously adjustable phase-control range of 360° and a frequency range from 5 to 6 GHz, a low transmission loss of 4 dB $\pm$ 1.7 dB is measured. The phase shifter is realized with a commercial 0.6-μm gallium–arsenide MESFET process and requires a chip area of only 0.8 mm^2. To the knowledge of the authors, the best results reported to date are reached for a continuously adjustable passive phase shifter with comparable circuit size. The presented circuit is well suited for wireless adaptive antenna transceivers, operating in accordance to the 802.11a, high-performance radio local-area-network and high-speed wireless-access-network type-a standards.**

***Index Terms*—Adaptive antenna combining, monolithic microwave integrated circuit (MMIC), phase shifter, varactor, wireless local area network (WLAN).**

I. Introduction

THE market forecasts for high-speed wireless local area networks (WLANs) are very promising [1]. Within the WLAN market, the 802.11a, high-performance radio local-area-network (HIPERLAN) and high-speed wireless-access-network type-a (HiSWANa) standards will play an important role in the U.S., Europe, and Japan, respectively. Adaptive antenna combining in the RF path is proposed to circumvent performance degradations caused by indoor multipath propagation [2].

Phase shifters are required for such adaptive antenna systems to set the phase of each antenna path. These phase shifters have to meet high requirements since they should have a continuously adjustable phase with a phase-control range of 360°, low transmission loss, low transmission-loss variation, low control complexity with single control voltage, adequate large-signal performance, and low or no dc power consumption. Furthermore, the phase shifters should be compact and low cost to enable commercial applications. In adaptive antenna receivers, the transmission loss and the transmission-loss variation can be compensated by the variable-gain low-noise amplifiers (VGLNAs) located in front of the phase shifters. Low power-consuming VGLNAs with a high-gain/dc-power-consumption figure-of-merit of up to 10 dB/mW have been reported in [3] and [4]. They have been fabricated on the same commercial GaAs MESFET technology as the phase shifter presented in this paper.

Many different passive and active phase-shifter monolithic microwave integrated circuits (MMICs) have been reported in literature [5]. A switched high-pass/low-pass phase shifter for the K-band with 5-bit resolution has been reported in [6]. This type of phase shifter has the advantage of not requiring digital-to-analog converters (DACs) for setting the control voltages. Unfortunately, this topology requires a large chip area and has a limited phase precision.

Active vector-modulator-based phase shifters (VMPSs) with very low power consumption [7], [8] and an ultra-compact passive VMPS [9] at the C-band have been presented. These VMPSs have a significant disadvantage. For 360° phase control, they need three control voltages, thereby having a high control complexity and requiring three costly and power-consuming DACs.

An active phase-shifter topology at the S-band using variable resonant circuits has been reported in [10]. Unfortunately, this phase shifter consumes a high dc power.

Ultra-compact phase shifters at the C-band with 210° and 360° phase-control range have been presented in [11] and [12], respectively, using the well-known reflective-type phase-shifter (RTPS) topology. The branch-line couplers have been substituted by lumped elements to minimize the circuit size. These circuits have relatively high losses, high-loss variations, and limited frequency bandwidths.

At the Ku-band, a phase-control range of 180° has been reached for an all-pass network-type phase shifter using two transmission lines with quarter-wavelength [13].

The loss variation of a K-band RTPS has been significantly reduced by using a complementary bias technique [14]. Unfortunately, this topology requires a relatively high control complexity and additional chip area.

Active inductors have been used for the reflective loads of an RTPS [15]. Very low loss and a phase-control range of 225° have been reached with this approach. However, significant disadvantages of this work are the high dc power consumption and the high noise figure.

A phase shifter with 360° phase control, low loss, low-loss variation, and high-frequency bandwidth has been realized with a varactor-loaded coplanar waveguide [16], which needs a relative large circuit area.

Microelectromechanical system (MEMS) technology has been applied for transmission-line phase shifters at the U- and W-band [17].

Manuscript received March 14, 2002; revised October 12, 2002.

F. Ellinger and H. Jäckel are with the Electronics Laboratory, Eidgenössische Technische Hochschule Zürich, Zürich CH-8092, Switzerland (e-mail: ellinger@ife.ee.ethz.ch).

W. Bächtold is with the Laboratory for Electromagnetic Fields and Microwave Electronics, Eidgenössische Technische Hochschule Zürich, Zürich CH-8092, Switzerland.

Digital Object Identifier 10.1109/TMTT.2003.809670

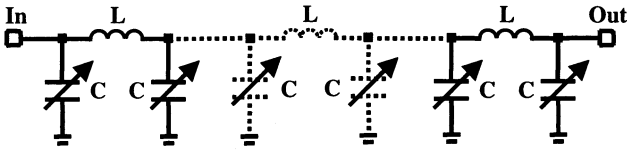

Fig. 1. Varactor-loaded transmission-line phase shifter using distributed low-pass structures realized by lumped elements. Neighboring varactor capacitances can be combined.

In order to significantly decrease the circuit size, the transmission line can be substituted by distributed low-pass structures consisting of lumped elements. A corresponding phase shifter with a phase-control range of 90° has been briefly presented in [18].

In this paper, the design procedure, optimization, and design tradeoffs of such varactor-loaded transmission-line phase shifters are elaborately discussed. An ultra-compact C-band MMIC phase shifter is presented to verify the proposed design considerations. Only one control voltage and one simple DAC is required to adjust the phase. A phase control of 360°, low loss, and excellent large-signal properties are reached using commercial low-cost GaAs technology. To the knowledge of the authors, the best performances reported to date are reached for a passive phase shifters with comparable size.

II. Theory

Phase control can be obtained by tuning the lumped-element equivalent of a transmission line. Distributed low- or high-pass structures in a T or Π configuration can be used for this purpose. The capacitance values can be easily varied by using common FET varactors. The inductor values could be varied by using active inductors, as reported in [15]. Unfortunately, active inductors consume high dc power and increase the circuit and control complexity, thereby limiting the suitability for wireless applications. Therefore, we focus on varactor-tuned transmission lines using spiral inductors with a fixed impedance.

Low-pass structures in a Π configuration, as shown in Fig. 1, are the best choice for that principle since they require a minimum number of area-consuming inductors. Neighboring varactor capacitances can be combined. Furthermore, the distributed phase shifter with Π low-pass structures allows minimum bias complexity. The anodes of the varactors are grounded without requiring additional bias circuitries. All cathodes of the varactors are connected by the inductors. Therefore, the control voltage has to be fed into only one inductor node of the whole distributed phase shifter. By varying the cathode voltage potential, a positive voltage can be applied within the main control range.

In the following, we want to investigate the characteristics of one Π low-pass element. The $ABCD$ matrix for the elements of the Π low-pass structure, normalized to the characteristic wave impedance Z_0, is given by [19]

$$\begin{vmatrix} \mathbf{A} & \mathbf{B} \\ \mathbf{C} & \mathbf{D} \end{vmatrix} = \begin{vmatrix} 1 & 0 \\ jY_C & 1 \end{vmatrix} \begin{vmatrix} 1 & jX_L \\ 0 & 1 \end{vmatrix} \begin{vmatrix} 1 & 0 \\ jY_C & 1 \end{vmatrix} \tag{1}$$

$$= \begin{vmatrix} 1 - Y_C X_L & jX_L \\ jY_C(2 - Y_C X_L) & 1 - Y_C X_L \end{vmatrix} \tag{2}$$

with

$$X_C = \frac{1}{Y_C} = \frac{1}{\omega C Z_0} \tag{3}$$

and

$$X_L = \frac{1}{Y_L} = \frac{\omega L}{Z_0} \tag{4}$$

as the normalized impedances of the capacitance and inductance, respectively. The transmission term S_{21} of the scattering matrix can be calculated by

$$S_{21} = \frac{2}{\mathbf{A} + \mathbf{B} + \mathbf{C} + \mathbf{D}} \tag{5}$$

$$= \frac{2}{2(1 - Y_C X_L) + j(X_L + 2Y_C - Y_C^2 X_L)}. \tag{6}$$

The corresponding transmission phase φ_{21}, which is equal to the characteristic length of a equivalent transmission line, can be calculated by

$$\varphi_{21} = \tan^{-1}\left[\frac{Y_C^2 X_L - 2Y_C - X_L}{2(1 - Y_C X_L)}\right]. \tag{7}$$

If we neglect resistive parasitics, lossless transmission and perfect match at the center operation frequency, f_o demands

$$|S_{11}| = \frac{\mathbf{A} + \mathbf{B} - \mathbf{C} - \mathbf{D}}{\mathbf{A} + \mathbf{B} + \mathbf{C} + \mathbf{D}} = 0 \tag{8}$$

and

$$|S_{22}| = \frac{-\mathbf{A} + \mathbf{B} - \mathbf{C} + \mathbf{D}}{\mathbf{A} + \mathbf{B} + \mathbf{C} + \mathbf{D}} = 0. \tag{9}$$

Solving of (8) or (9) gives

$$\mathbf{B} = \mathbf{C} \tag{10}$$

since $\mathbf{A} = \mathbf{D}$, as shown in (2). Thus, we get

$$X_{L,0} = \frac{2Y_{C,0}}{1 + Y_{C,0}^2} \tag{11}$$

with the inductor impedance $X_{L,0}$ and the center capacitor admittance $Y_{C,0}$ at f_o. Using (11) and (7) gives

$$Y_{C,0} = -\tan\left(\frac{\varphi_{21,0}}{2}\right). \tag{12}$$

The center transmission phase $\varphi_{21,0}$ is the transmission phase obtained at $X_{L,0}$ and $Y_{C,0}$. By using (12) and (11), we get

$$X_{L,0} = -\sin(\varphi_{21,0}). \tag{13}$$

For our low-pass structure, (12) and (13) are valid for $0 \geq \varphi_{21,0} \geq -90$. The impedance $X_{L,0}$ is fixed, whereas Y_C can be varied from $Y_{C\min}$ to $Y_{C\max}$ with the capacitance-control ratio

$$r_C = \frac{C_{\max}}{C_{\min}} = \frac{Y_{C\max}}{Y_{C\min}}. \tag{14}$$

To reach a symmetrical variation of Y_C around $Y_{C,0}$, we can define

$$Y_{C\max} = Y_{C,0}\sqrt{r_C} \tag{15}$$

and

$$Y_{C\min} = \frac{Y_{C,0}}{\sqrt{r_C}} \tag{16}$$

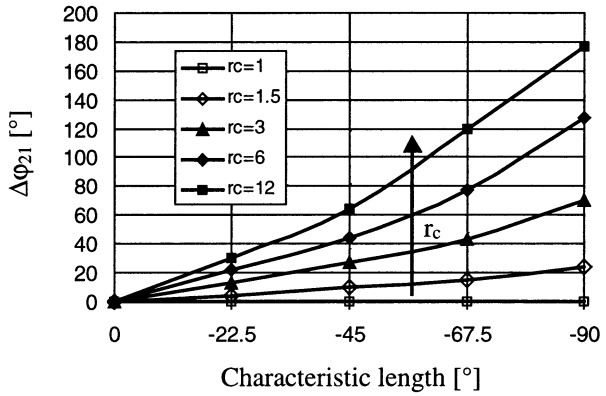

Fig. 2. Transmission phase-control range $\Delta\varphi_{21}$ versus characteristic length $\varphi_{21,0}$ capacitance-control range r_C at the center operation frequency of one low-pass section assuming ideal elements.

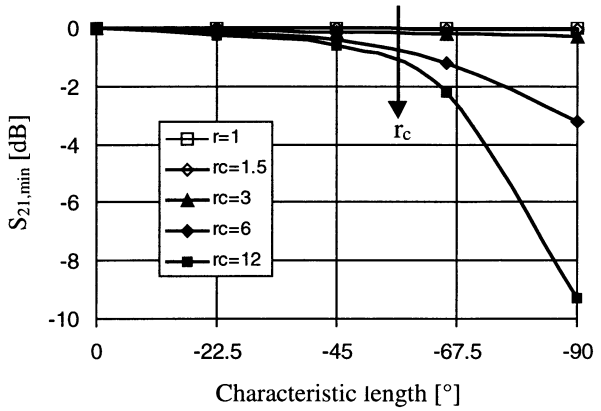

Fig. 3. Maximum transmission loss $S_{21,\min}$ due to reactive mismatch versus characteristic length $\varphi_{21,0}$ and capacitance-control range r_C at the center operation frequency of one low-pass section assuming ideal elements.

which is a good compromise between high transmission phase-control range and low transmission loss due to reactive mismatch. The phase-control range of one ideal Π low-pass section is then given by

$$\Delta\varphi_{21} = \left|\varphi_{21}(Y_{C\max}) - \varphi_{21}(Y_{C\min})\right| \tag{17}$$

$$= \left| \tan^{-1}\left[\frac{Y_{C,0}^2 r_C X_{L,0} - 2Y_{C,0}\sqrt{r_C} - X_{L,0}}{2\left(1 - Y_{C,0}\sqrt{r_C}X_{L,0}\right)}\right] - \tan^{-1}\left[\frac{\dfrac{Y_{C,0}^2 X_{L,0}}{r_C} - \dfrac{2Y_{C,0}}{\sqrt{r_C}} - X_{L,0}}{2\left(1 - \dfrac{Y_{C,0}X_{L,0}}{\sqrt{r_C}}\right)}\right]\right|. \tag{18}$$

The transmission phase-control range versus capacitance-control ratio and center transmission phase is illustrated in Fig. 2.

The phase-control range is increasing with increasing characteristic length, demanding increasing values of the lumped capacitances and inductances, as shown in (12) and (13). In this case, the resonance frequency of the structure

$$\omega_r = \frac{1}{\sqrt{\mathrm{LC}}} \tag{19}$$

around which maximum phase variations are obtained is decreasing. Thus, the distance between the operation and resonance frequencies is decreasing. Unfortunately, close or above the resonance frequency, the signal is attenuated due to the low-pass characteristics. Therefore, a compromise between maximum transmission phase-control range and minimum transmission loss has to be found for a given capacitance-control range. The minimum transmission loss $S_{21,\max}$, obtained at f_0 and $\varphi_{21,0}$, equals zero because ideal elements are assumed. Due to the reactive mismatch, transmission loss is created. The maximum transmission loss is obtained at $Y_{C\max}$ since the low-pass effect of the structure is maximum at maximum capacitance

$$S_{21,\min} = S_{21}(Y_{C\max}). \tag{20}$$

Using (6) gives the relation

$$S_{21,\min} = \frac{2}{\sqrt{4\left(1 - Y_{C\max}X_{L,0}\right)^2 + \left(X_{L,0} + 2Y_{C\max} - Y_{C\max}^2 X_{L,0}\right)^2}}. \tag{21}$$

With (15) and (16), we can write (22), shown at the bottom of this page. For the maximum transmission-loss variation, we can write

$$\Delta S_{21} = \left|S_{21,\max} - S_{21,\min}\right| = \left|S_{21,\min}\right|. \tag{23}$$

The maximum transmission loss versus characteristic length and capacitance-control range is shown in Fig. 3.

III. MMIC Design

A phase shifter at the C-band was designed to verify the proposed phase-shifter principle. A characteristic length of approximately -50° at the center frequency of 5.5 GHz was chosen for each low-pass element since this value is a good compromise between low loss and high phase control for capacitance-control ranges typically provided by common MESFET varactors. At a capacitance-control ratio of three, the theoretical transmission phase-control range and transmission loss of one element are approximately 30° and 0.15 dB, respectively. The required inductor and center capacitance values for a characteristic wave impedance of 50 Ω are approximately 1.2 nH and 0.3 pF, respectively. They were calculated using (3), (4), (12), and (13). In practice, the capacitance-control ratio and transmission phase control are degraded by the capacitive parasitics of the inductors. Beside the low-pass characteristics of the lumped-element

$$S_{21,\min} = \frac{2}{\sqrt{4\left(1 - Y_{C,0}\sqrt{r_C}X_{L,0}\right)^2 + \left(X_{L,0} + 2Y_{C,0}\sqrt{r_C} - Y_{C,0}^2 r_C X_{L,0}\right)^2}} \tag{22}$$

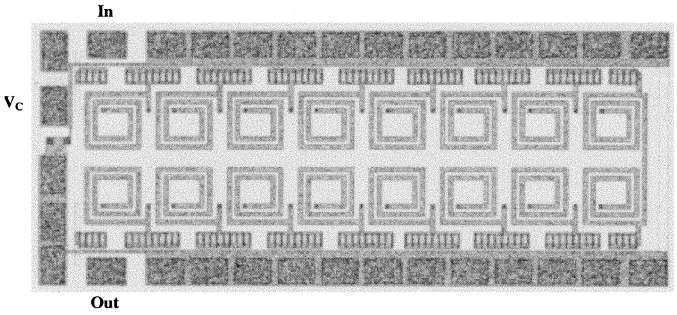

Fig. 4. Varactor-tuned transmission-line phase shifter consisting of 16 lumped low-pass elements in a Π configuration. Chip size is 1.4 mm × 0.6 mm.

equivalent of the transmission line, the transmission loss is determined by the quality factors of the inductors and varactors.

The circuit was fabricated using the commercial Triquint TQTRx GaAs MMIC process, featuring MESFETs with gate lengths of 0.6 μm and transit frequencies around 18 GHz. Deep depletion-type FETs (G-FETs), which provide a capacitance-control ratio of approximately three, are used as varactors. A relatively high number of 16 cascaded low-pass elements was used to guarantee a phase shift of 360° within a sufficient frequency bandwidth. The dc control voltage V_C is fed into one inductor node by using a high-ohmic resistor, thereby connecting all cathodes of the varactors. The anodes of the varactors are grounded. The quality factor Q of the varactors are increasing with increasing V_C. At 5.5 GHz and control voltages of 0 and 5 V, the quality factors are around 14 and 32, respectively. The Q of the inductors is approximately 23.

A inductor–resistor–capacitor (LRC) Π-type equivalent circuit was used to model the inductors. The varactors were modeled using a simple series connection of a voltage-controlled capacitor and a voltage-controlled resistor. The grounding connections have a strong influence on the phase characteristics. They have been simulated using a simple transmission-line model.

A photograph of the MMIC chip having a chip size of only 1.4 mm × 0.6 mm is shown in Fig. 4. The GaAs chip costs of one circuit in mass fabrication are approximately 0.6 US$.

IV. Results of MMIC Phase Shifter

The circuit was measured on-wafer using an HP 8510B network analyzer. The measured and simulated transmission phase control, transmission loss, and return losses are shown in Figs. 5–7, respectively. Excellent results are obtained from 4.5 to 6.5 GHz.

Within a measured phase-control range of 360°, the measured transmission losses at 4.5, 5.5, and 6.5 GHz are 3.6 dB ± 1.8 dB ($V_C = -0.4$ V,…, 5 V), 3.9 dB ± 1.5 dB ($V_C = -0.25$ V,…, 5 V), and 4.5 dB ± 1.6 dB ($V_C = 0.1$ V,…, 5 V). The transmission loss and phase-control range are increasing with increasing frequency since the distance between the operation and resonance frequencies is decreasing. Thus, the low-pass effect is increasing. A similar effect can be found for decreasing V_C since the capacitance is increasing and the low-pass effect is also increasing.

The measured return losses are higher than 10 dB. A 1-dB input compression point of higher than 12 dBm was measured.

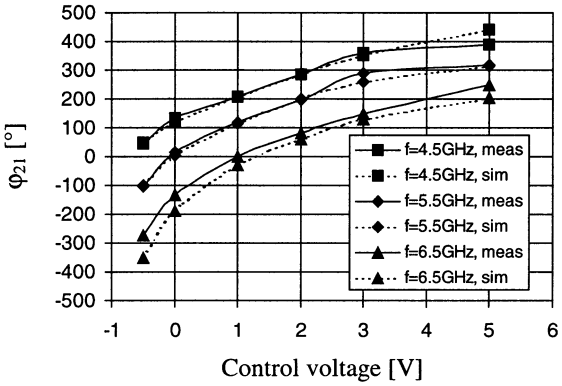

Fig. 5. Measured transmission phase versus control voltage and operation frequency of the phase shifter.

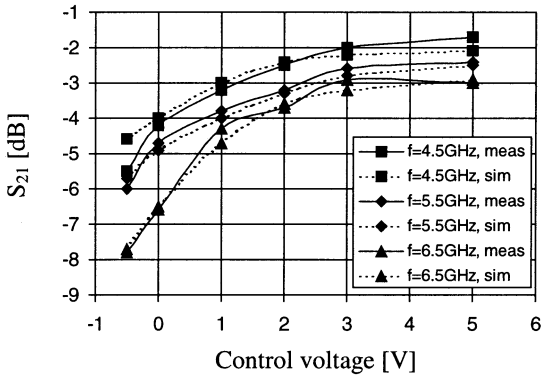

Fig. 6. Measured transmission loss versus control voltage and operation frequency of the phase shifter.

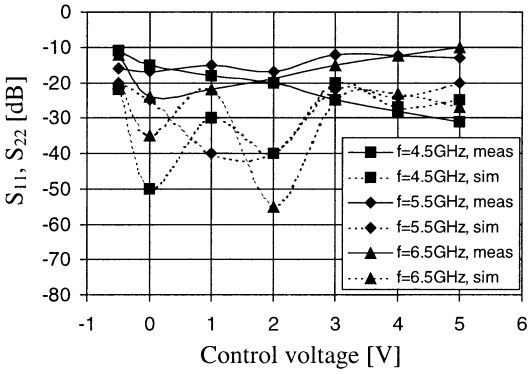

Fig. 7. Measured return losses ($S_{11} = S_{22}$) versus control voltage and operation frequency of the phase shifter.

TABLE I
Calculation Assuming Ideal Elements, Simulation, and Measurement of Phase-Control Range and Maximum Transmission Loss at 5.5 GHz

	Ideal Calculation	*Simulation*	*Measurement*
Phase control range	480°	415°	410°
Maximum transmission loss	2.4dB	5.7dB	6dB

The control linearity (function of phase versus control voltage) is good, keeping the resolution requirements and costs for the DAC low.

Good agreement between the measured and simulated results are obtained for the transmission phases and transmission losses.

TABLE II
COMPARISON OF CONTINUOUSLY ADJUSTABLE PHASE-SHIFTER MMICS

Ref.	*Phase control*	*Band-width*	*Gain/ Ripple*	*Power supply*	*Control voltages*	*Circuit area/ Technology*	*Principle*
[18]	90°	4GHz-6GHz	-1.2dB ± 0.5dB	~0mW	1	0.5mm^2 0.6µ GaAs MESFET	Lumped element transmission line PS
[14]	90°	40GHz-60GHz	-4dB ± 0.4dB	~0mW	2	1.5mm^2 0.3µ GaAs PHEMT	RTPS with complementary bias
[13]	180°	12GHz-14GHz	-3.6dB ± 1.1dB	~0mW	1	3mm^2 0.3µ GaAs MESFET	All pass network type PS using two λ/4 lines
[11]	210°	6.1GHz-6.3GHz	-5.3dB ± 1.4dB	~0mW	1	0.9mm^2 0.6µ GaAs MESFET	RTPS
[15]	225°	4.7GHz-6.7GHz	-0.6dB ± 0.2dB	>100 mW	1	0.1mm^2 0.1µ InP HEMT	RTPS using active inductors
[16]	360°	5GHz-20GHz	-4.4dB ± 0.6dB	~0mW	1	n. a. large GaAs Schottky Diode	Tuned CPW PS
[10]	360°	2.38GHz-2.42GHz	2dB ± 0.7dB	>90mW	2	2.3mm^2 0.3µ GaAs MESFET	Active variable resonant circuit
[7]	360°	4.8GHz-5.8GHz	0dB n.a.	9mW	3	2.4mm^2 0.6µ GaAs MESFET	Active vector modulator
[8]	360°	5.1GHz-5.3GHz	0.6dB n.a.	10mW	3	1.3mm^2 0.6µ GaAs MESFET	Active vector modulator
[9]	360°	4.7GHz-5.7GHz	-9dB n.a.	~0mW	3	1mm^2 0.6µ GaAs MESFET	Passive vector modulator
[12]	360°	5.15GHz-5.7GHz	-6.4dB ± 3dB	~0mW	1	0.9mm^2 0.6µ GaAs MESFET	RTPS
[17]	360°	75GHz-110GHz	-5dB n.a.	~0mW	1	n.a. MEMS	Distributed transmission line PS
This work	**360°**	**5GHz-6GHz**	**-4dB ± 1.7dB**	**~0mW**	**1**	**0.8mm^2 0.6µ GaAs MESFET**	**Lumped element transmission line PS**

A comparison of the calculated, simulated, and measured phase-control range and the maximum loss is shown in Table I. Again, we can see the good agreement between simulation and measurement. For the ideal calculation, as discussed in Section II, the varactors and inductors have been assumed to be ideal. Thus, only the transmission loss due to the reactive mismatch is considered. Due to the resistive parasitics of the varactors and inductors, the measured maximum transmission loss is higher than the calculated one. Furthermore, the measured phase-control range is smaller than the simulated one since the effective capacitance-control range of the varactors is decreased by the parasitic capacitances of the inductors.

In Table II, key results of this study are compared with other studies using different active and passive topologies. In comparison, the phase shifter presented in this study has excellent performances and requires only a small circuit area.

V. CONCLUSION

The design of a varactor-loaded transmission-line phase shifter using lumped elements has been discussed in this paper.

An ultra-compact MMIC phase shifter at the C-band has been realized to verify the proposed topology and design procedure. The passive MMIC allows a continuously adjustable phase control of 360° with only one control voltage within a frequency range from 4.5 to 6.5 GHz. A low transmission loss with moderate loss variation and excellent large-signal performances have been measured. The control linearity is good, keeping the requirements for the DAC low. To the knowledge of the authors, the best performances reported to date have been reached for a passive phase shifter with comparable size.

Due to its excellent performance, simple design, low chip costs, and low control complexity, the presented C-band phase shifter is very well suited for commercial applications. The MMIC is a potential candidate for wireless adaptive antenna transceivers, operating in accordance to the 802.11a, HIPERLAN, and HiSWANa standards.

ACKNOWLEDGMENT

The authors would like to thank R. Vogt and T. Brauner, both of the Laboratory for Field Theory and Microwave Electronics, Eidgenössische Technische Hochschule (ETH) Zürich, Zürich, Switzerland, for kindly providing the circuit area on their wafer run for the MMIC presented in this paper. Furthermore, the authors would like to acknowledge L. Rodoni, Electronics Laboratory, ETH Zürich, for the fruitful discussions concerning this study. Finally, the authors would like to thank the unknown reviewers for their helpful and constructive comments.

REFERENCES

[1] "WLAN chipset market—The incredible journey is just beginning," In-Stat/MDR, Res. Rep. IN020271WT, 2002.
[2] A. Wittneben, "Smart antennas for low cost wireless communications," *Frequenz*, vol. 54, no. 1–2, pp. 58–64, Jan.–Feb. 2000.
[3] F. Ellinger, U. Lott, and W. Bächtold, "Ultra low power GaAs MMIC low noise amplifier for smart antenna combining at 5.2 GHz," in *IEEE Radio Frequency Integrated Circuit Symp.*, June 2000, pp. 157–159.
[4] ——, "A 5.2 GHz variable gain LNA MMIC for adaptive antenna combining," in *IEEE MTT-S Int. Microwave Symp. Dig.*, vol. 2, June, pp. 87–89.
[5] S. K. Koul and B. Bhat, *Microwave and Millimeter Waver Phase Shifters*. Norwood, MA: Artech House, 19??, vol. II.
[6] C. F. Campell and S. A. Brown, "A compact 5-bit phase-shifter MMIC for K-band satellite communication systems," *IEEE Trans. Microwave Theory Tech.*, vol. 48, pp. 2652–2656, Dec. 2000.

[7] F. Ellinger, U. Lott, and W. Bächtold, "A calibratable adaptive antenna combiner at 5.2 GHz with high yield for PCMCIA card integration," *IEEE Trans. Microwave Theory Tech.*, vol. 48, pp. 2714–2720, Dec. 2000.
[8] ——, "An antenna diversity MMIC vector modulator for HIPERLAN with low power consumption and calibration capability," *IEEE Trans. Microwave Theory Tech.*, vol. 49, pp. 964–969, May 2001.
[9] F. Ellinger, R. Vogt, and W. Bächtold, "A high yield, ultra small, passive, vector modulator based phase shifter for smart antenna combining at C-band," in *IEEE/CSIRO Asia–Pacific Microwave Conf.*, Sydney, Dec. 2000, pp. 794–797.
[10] H. Hayashi and M. Muraguchi, "An MMIC active phase shifter using a variable resonant circuit," *IEEE Trans. Microwave Theory Tech.*, vol. 47, pp. 2021–2026, Oct. 1999.
[11] F. Ellinger, R. Vogt, and W. Bächtold, "Compact reflective type phase shifter MMIC for C-band using a lumped element coupler," *IEEE Trans. Microwave Theory Tech.*, vol. 49, pp. 913–917, May 2001.
[12] ——, "Ultra compact reflective type phase shifter MMIC at C-band with 360° phase control range for smart antenna combining," *IEEE J. Solid-State Circuits*, vol. 37, pp. 481–486, Apr. 2002.
[13] H. Hayashi, T. Nakagawa, and K. Araki, "A miniaturized MMIC analog phase shifter using two quarter-wave-length transmission lines," *IEEE Trans. Microwave Theory Tech.*, vol. 50, pp. 150–154, Jan. 2002.
[14] S. Nam, A. W. Payne, and I. D. Robertson, "RF and microwave phase shifter using complementary bias techniques," *Electron. Lett.*, vol. 37, no. 18, pp. 1124–1125, Aug. 2001.
[15] H. Hayashi, M. Muraguchi, Y. Umeda, and T. Enoki, "A high-Q broad-band active inductor and its application to a low-loss analog phase shifter," *IEEE Trans. Microwave Theory Tech.*, vol. 44, pp. 2369–2374, Dec. 1996.
[16] A. S. Nagra and R. A. York, "Distributed analog phase shifters with low insertion loss," *IEEE Trans. Microwave Theory Tech.*, vol. 47, pp. 1705–1711, Sept. 1999.
[17] N. S. Barker and G. M. Rebeiz, "Optimization of distributed MEMS transmission-line phase shifters—U-band and W-band designs," *IEEE Trans. Microwave Theory Tech.*, vol. 48, pp. 1957–1966, Nov. 2000.
[18] F. Ellinger, R. Vogt, and W. Bächtold, "Ultra compact, low loss, varactor tuned phase shifter MMIC at C-band," *IEEE Microwave Wireless Comp. Lett.*, vol. 11, pp. 104–105, Mar. 2001.
[19] R. V. Garver, "Design equations and bandwidth of loaded line phase shifters," *IEEE Trans. Microwave Theory Tech.*, vol. MTT-22, pp. 561–563, May 1974.

Frank Ellinger (S'97–M'02) was born in Friedrichshafen, Germany, in 1972. He received the Masters degree in electrical engineering from the University of Ulm, Ulm, Germany, in 1996, and the Masters degree in business and administration and Ph.D. degree in electrical engineering from the Eidgenössische Technische Hochschule (ETH) Zürich, Zürich, Switzerland, in 2001.

During his MBA studies in 2001, he was with the Wireless Marketing Division, Infineon, Munich, Germany. Since 2001, he has been Head of the RFIC Design Group, Electronics Laboratory, ETH, and Project Leader of the IBM/ETH Competence Center for Advanced Silicon Electronics. His main interests are the characterization, modeling and design of silicon and GaAs-based RF circuits for high-speed wireless and optical communication. He has authored over 20 IEEE papers.

Dr. Ellinger was the recipient of the Young Ph.D. Award of the ETH (Bonus 29), the ETH Medal for outstanding Ph.D. theses, and the Denzler Award of the Swiss Electrotechnical Association (SEV).

Heinz Jäckel (M'82) received the Doctorate degree in electrical engineering from the Eidgenössische Technische Hochschule (ETH) Zürich, Zürich, Switzerland, in 1979.

In 1980, he joined IBM, where he held scientific and management positions for 13 years in the Research Laboratories in Rüschlikon, Switzerland, and Yorktown Heights, NY. During this time, he carried out research projects in the field of device and circuit design for superconducting Josephson junction computers, GaAs-MESFET logic and memory integrated circuits (ICs), and optoelectronics. In 1988, he was instrumental in the establishment of the opto-electronic project at IBM, where he subsequently managed the optical storage devices activities. Since 1993, he has been a Full Professor of analog electronics with the Electronics Laboratory, ETH Zürich. The research activities of his High Speed Electronics and Photonics Group at ETH concentrate on the following topics: technology, design, and characterization of ultrafast transistors (mainly InP-based HBTs) and circuits for multiten gigabit electronics, IC design of RF circuits for mobile communication and CMOS-ASICs for sensory technology. In the area of lightwave communication, his group pursues research on photonic devices and integrated optical circuits for data transmission, particularly InP-based all-optical devices for all optical signal processing at terabit/s data rates.

Werner Bächtold (M'71–SM'99–F'00) was born October 1, 1939. He received the Diploma degree and Ph.D. degree in electrical engineering from the Eidgenössische Technische Hochschule (ETH), Zürich, Switzerland, in 1964 and 1968, respectively.

From 1969 to 1987, he was with the IBM Zürich Research Laboratory, where he was involved with device and circuit design and analysis of GaAs MESFETs, design of logic and memory circuits with Josephson junctions, and semiconductor lasers for digital communication. He was on assignment with the IBM T. J. Watson Research Center, Yorktown Height, NY. Since December 1987, he has been a Professor of electrical engineering with the ETH. He heads the Microwave Electronics Group, Laboratory for Electromagnetic Fields and Microwave Electronics. He is engaged with design and characterization of MMICs, design and technology of InP-high electron-mobility transistor (HEMT) devices and circuits, as well as microwave photonics.